

# SIMULATION OF STRONG GROUND MOTION FOR NORTH-EASTERN REGION OF INDIA

**Babita Sharma\***  
MEE16702

**Supervisor: Hiroe MIYAKE\*\*  
Toshiaki YOKOI\*\*\*  
Takumi HAYASHIDA\*\*\***

## ABSTRACT

Earthquakes are the most unpredictable among all the natural disasters. The regions experienced great earthquakes in the past are most probable candidates for the future major/great earthquakes. Therefore, in this study, the north-eastern region of India has been chosen to simulate strong ground motion for a hypothetical major earthquake (Mw 7.0) using the empirical Green's function method. Recordings of the 2009 Bhutan earthquake (Mw 5.1 and 6.1) are considered as empirical Green's functions with a characterized source model with asperity. Source scaling for the validation of the technique was accomplished by simulation of the Mw 6.1 event using recordings of the Mw 5.1 earthquake with the fault extended to Mw 7.0. As a result, it was observed that cities in the north-eastern region of India will exhibit peak ground acceleration (PGA) for a maximum of 121 gals in the case of a major earthquake of Mw 7.0. Sites located near the rupture initiation point/scenarios can expect higher level accelerations. For validation, estimates of the PGA for the Mw 7.0 simulation were compared with predictive ground motion equations for the Himalayan region with comparable PGA estimates. The obtained PGA values have provided an idea about the level of accelerations experienced in the area for a hypothetical, and probable, future Mw 7.0 earthquake. With the data of ground motions and PGA values obtained in the present analysis, future construction in the area can be regulated and built environments strengthened accordingly.

**Keywords:** Simulation, Peak Ground Acceleration, Strong Motion Generation Area, Background Area.

## 1. INTRODUCTION

The Indian subcontinent is unique because of the continent-continent collision of the Indian plate with the Eurasian plate. Due to this collision, the inter-plate region comprised of the entire 2500 km Himalayan belt from west to east is seismically active. The collision of the Indian and the Eurasian plates results in crustal shortening along the northern edge of the Indian plate due to which three major thrust planes, i.e. the Main Frontal Thrust (MFT), the Main Boundary Thrust (MBT), and the Main Central Thrust (MCT), have formed (Gansser, 1964; Molnar and Chen, 1982). No great earthquake has occurred in the Himalaya since 1950 (Khatttri, 1999; Bilham and Gaur, 2000). The recurrence of similar or larger earthquakes has been the most discussed issue in the Himalayan region. There are several seismic gaps in the entire Himalayan belt where segments of an active fault have not slipped for long periods of time compared to other segments (Bilham and Wallace, 2005; Gupta and Gahalaut, 2014). Therefore, it is required to have the idea of the ground motions from the future probabilistic earthquakes. In the present study, empirical Green's function (EGF) method to simulate strong ground motions,

---

\*National Centre for Seismology, Ministry of Earth Sciences, New Delhi, India.

\*\*Earthquake Research Institute, The University of Tokyo, Tokyo, Japan.

\*\*\*International Institute of Seismology and Earthquake Engineering, Building Research Institute, Tsukuba, Japan.

proposed by Irikura (1986), has been utilized for the north-eastern Indian region to simulate scenario earthquake of Mw 7.0. The source characterization for the same is accomplished using recipe of strong ground motion given by Miyake et al. (2003). The 2009 Bhutan earthquake and its aftershock recorded in north-eastern region of India are used for the purpose. This study will be useful for this region because most of the cities in this region have undergone phenomenal socio-economic growth.

## 2. DATA

Strong Motion Accelerographs (SMA) network installed in the north-eastern region of India comprised of 50 stations. This network was funded by Ministry of Earth Sciences and operated by IIT, Roorkee and National Centre for Seismology. This network is in operation after 2008. The SMA's consist of internal AC-63 GeoSIG triaxial force-balanced accelerometers and GSR-18 GeoSIG, 18-bit digitizers with external GPS. The recording for all instruments is in trigger mode at a sampling frequency of 200 samples per second. The recording is done on a 256 MB GeoSIG or 1-GB Kinematics compact flash card and the instruments are installed in different geological conditions.

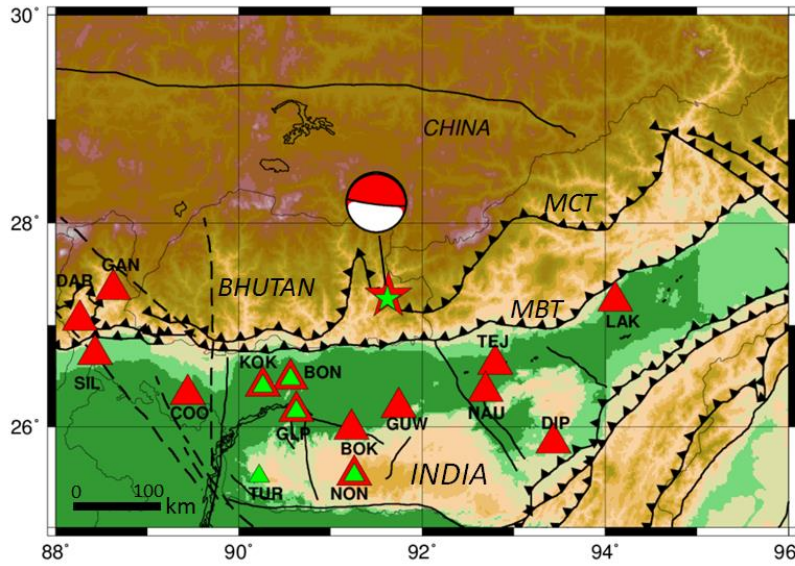


Figure 1. The 2009 Bhutan earthquake (red star and fault plane solution) and its aftershock (green star) recorded in the north-eastern region of India. Red triangles triggered by the Bhutan earthquake and green triangles by aftershock.

The 2009 Bhutan earthquake (Mw 6.1) along with its aftershock (Mw 5.1) have been chosen as the possible candidates for the simulation of strong ground motion as shown in Figure 1. The Mw 6.1 main shock has been recorded by 14 stations scattered in the area. The aftershock of this earthquake was recorded at five stations. Four stations have recorded both earthquakes and one station has only recorded the aftershock. These four stations data have been used to validate the EGF's method for the region and after that Mw 6.1 is used as an element earthquake to simulate Mw 7.0 and estimated peak ground acceleration (PGA) for the north-eastern region of India.

## 3. THEORY AND METHODOLOGY

### 3.1. Outer Fault Parameters

The outer fault parameters are comprised of entire rupture area ( $S$ ) and total seismic moment ( $M_0$ ). The average stress drop ( $\sigma_c$ ) are related through the empirical relations given in Equations 1 and 2.  $R$  is the radius of circular fault and  $r$  is the radius of asperity (Irikura and Miyake, 2011).

$$M_0 = \frac{16}{7\pi^{1.5}} \sigma_c S^{1.5} \quad (1)$$

$$\sigma_c = \frac{7 M_0}{16 r^2 R} \quad (2)$$

### 3.2. Inner Fault Parameters and Empirical Green's Function Method

The inner fault parameters are slip heterogeneity inside the source, area of asperities, and stress drop on each asperity. Seismic activity is lower inside asperities and relatively higher surrounding the asperities. Combined area of asperity is 22 % of the total fault area for inland earthquakes (Somerville et al., 1999) and 25 % for subduction earthquakes. To estimate the combined area of asperity and the number of asperities, scaling relations can be used. After that, stress drop on each asperity ( $\sigma_a$ ) can be estimated through the relationship given in Equation 3 for the multi-asperity model. In this equation  $S_a$  is the area of asperity which is also called strong motion generation area.

$$\sigma_a = \sigma_c \frac{S}{S_a} \quad (3)$$

The equations used to synthesize a large event using small earthquakes given by Irikura et al. (1997), are written as below:

$$U(t) = \sum_{i=1}^N \sum_{j=1}^N (r/r_{ij}) \cdot F(t) * (C \cdot u(t))$$

$$F(t) = \delta(t - t_{ij}) + \left\{ 1/n' (1 - \exp(-1)) \right\} \times$$

$$\sum_{k=1}^{(N-1)n'} \left[ \exp\left\{ -(k-1)/(N-1)n' \right\} \cdot \delta\left\{ t - t_{ij} - (k-1)T/(N-1)n' \right\} \right] \quad (4)$$

where  $U(t)$ : synthesized waveform (large event),  $u(t)$ : observed element waveform,  $N$ : moment ratio of large/ small event,  $T$ : rise time of large event,  $C$ : stress drop of large/small event  $r$ : the hypocentral distance from observation point to the subevent,  $r_{ij}$ : the distance from the observation point to the sub fault with  $i$ th row and  $j$ th column,  $t$ : the rise time from observation point to subfault,  $t_{ij}$ : the rise time divided by the number of subfaults,  $n'$ : an appropriate integer to eliminate spurious periodicity and  $*$ : convolution.

## 4. RESULTS AND DISCUSSION

### 4.1. First Step Simulation

Figure 2 shows the strong motion generation area obtained to synthesize Mw 6.1 from the Mw 5.1 event data. Figure 3 shows the simulated waveforms, and observed and element earthquake waveforms for BON (EW component). The source dimensions of length 2.2 km, width 1.8km, rise time 0.1 sec and rupture initiation (1, 3) were chosen on the basis of iterations performed until the residual approached zero and correlation approached 1.

Table 1. Parameters used for observed and simulated earthquake for the simulation of Mw 6.1 event using Mw 5.1 data and Mw 7.0 using Mw 6.1 data.  $M_0$  is seismic moment and  $V_r$  is rupture velocity.

Element Earthquake	Middle Earthquake	Target Earthquake
Bhutan Earthquake (aftershock)	Bhutan Earthquake (main shock)	Hypothetical Major Earthquake (Mw 7.0)
$M_0 = 5.62 \times 10^{16}$ Nm	$M_0 = 1.78 \times 10^{18}$ Nm	$M_0 = 3.98 \times 10^{19}$ Nm
Depth=5 km (source)	Depth=8 km	Depth=15 km and 19 km
Strike=293°, Dip=7° and Slip=107°	Strike=281°, Dip=6° and Slip=94°	Source1: Strike=298°, Dip=6° and Slip=94° Source2: Strike=290°, Dip=10° and Slip=94°
$V_r = 3.0$ km/s, Rise time = 0.3 for Mw6.1 and 0.9 for Mw 7.0		

## 4.2. Second Step Simulation

After validating the EGF method for the north-eastern region of India, a hypothetical earthquake was simulated using Mw 6.1 data for fifteen stations in the target area. The source parameterization of the first step simulation was extended to make it a source for Mw 7.0 for the second step simulation using the formulations given by Irikura and Miyake (2011).

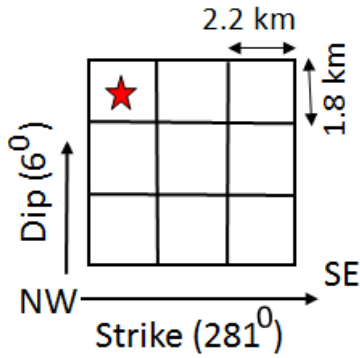


Figure 2. Strong motion generation area estimated by source parameterization to synthesize Mw 6.1 using Mw 5.1 event data, with parameters of source dimension, rupture initiation point (red star), strike and dip angles.

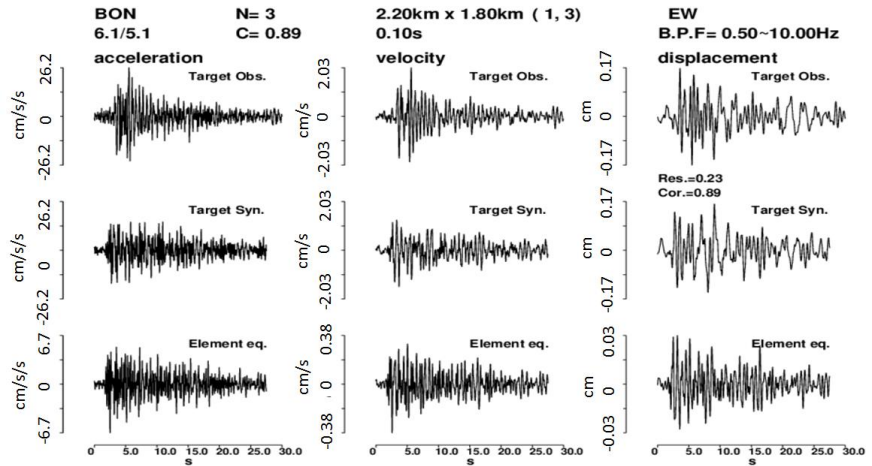


Figure 3. Target observed earthquake (Mw 6.1), target synthetic, and element observed earthquake (Mw 5.1) waveforms for acceleration, velocity, and displacement recorded at BON station (EW component).

The fault was positioned for two cases (target 1 and target 2) in the region according to seismotectonics and available fault plane solution as shown in Figure 4. The red rectangle within the fault is the asperity for a major earthquake of Mw 7.0 which can be considered the strong motion generation area (SMGA). The two red stars (small) in Figure 4 are the scenarios N1 and N2 for target 1 and S1 and S2 for target 2 cases. The geometry of the fault is shown in Figure 5 and radial propagation of the wave is considered for the present study. Using this fault model and the Mw 6.1 earthquake recorded in the region, the scenario earthquake (Mw 7.0) is simulated at fourteen sites in the region. The waveform histories obtained at these sites for the scenario earthquake and the PGA values for all the sites are estimated.

The comparisons of simulated PGA values with the ground motion prediction equation (GMPE) by Sharma et al. (2009) show PGA tended to decrease with respect to distance (Figures 6 and 7). The dark line is for the validity of the GMPE upto 200 kms and after that PGA is extended based on the same relation which is shown by dashed line after solid line. On the other hand it is important to note that at lesser distances, few PGA values are overestimated than the GMPE and at greater distances also few PGA values are smaller than the GMPE as shown in Figures 6 and 7. This may be due to the effect of rupture directivity and site amplification of ground motions which are not included in the GMPE for lesser distances. The GMPE is valid up to 200 km of fault distance, therefore further investigation of ground motion attenuation is needed for greater distances by introducing more data.

This study is an attempt to estimate deterministic seismic hazard assessment for the north-eastern region of India using the 2009 Bhutan earthquake. The level of ground accelerations expected in this region for a hypothetical major Mw 7.0 earthquake have been ascertained. Due to the socio-economic importance of this region and the prevalence of poor construction practices, there is an urgent need to assess seismic hazard in this area. It is hoped, therefore, that this study may prove useful for assessing seismic hazard in the target area.

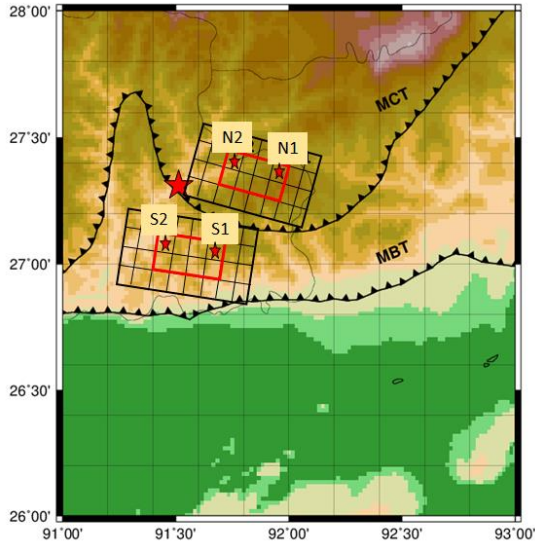


Figure 4. Schematic presentation of two targets with scenarios positioned in the area.

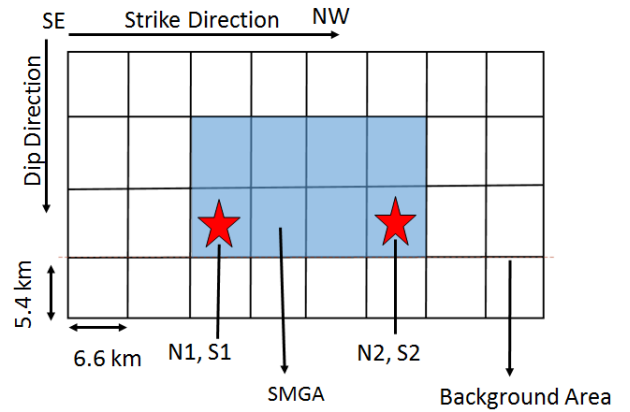


Figure 5. Characterized source model to simulate Mw 7.0 with SMGA (light blue color), background area (white color), and hypocenter scenarios (N1 & N2)/(S1 & S2) for two targets.

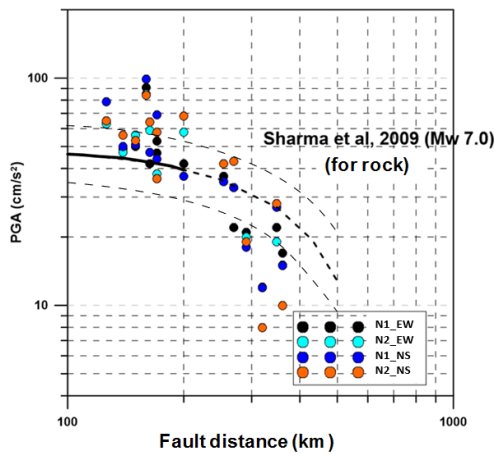


Figure 6. Comparison of calculated PGA values for target 1 (N1 & N2) cases using EW and NS components with the GMPE by Sharma et al. (2009) for Mw 7.0, which is valid for the Himalayan region. Above and below dashed lines are  $\pm 1$  standard deviation.

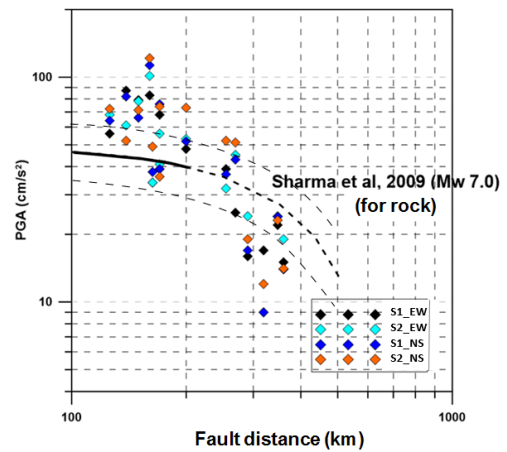


Figure 7. Comparison of calculated PGA values for target 2 (S1 & S2) cases using EW and NS components with the GMPE by Sharma et al. (2009) for Mw 7.0 which is valid for the Himalayan region. Above and below dashed lines are  $\pm 1$  standard deviation.

## 5. CONCLUSIONS

In the present study, the EGF approach has been utilized to model a major earthquake of Mw 7.0 using observed ground motions for the 2009 Bhutan earthquake (Mw 6.1) and its aftershock (Mw 5.1) which occurred in close proximity of the Bhutan Himalaya. The level of ground motions for the Mw 7.0 earthquake are compared with ground motion prediction equation for Himalayan region. It has been

observed that PGA values are found to be comparable to the ground motion prediction equation with respect to distance. The present study using the EGF methodology has provided constraints on the level of accelerations experienced during a scenario earthquake of Mw 7.0 and its impact in north-eastern region of India. It has been observed that the towns near to the rupture initiation may have experienced large ground accelerations during Mw 7.0 and the whole region may expect acceleration in excess of 100 gals. This study is important in socio-economic point of view because ground motions estimated here are helpful for the engineering community for planning future construction and retrofitting existing structures in the region.

## **6. RECOMMENDATION**

The simulation of strong ground motion can be extended to perform in the Indo-Myanmar region, Central Himalayan region of India and a seismic hazard map in a deterministic way should be prepared by using more data of small earthquakes as element earthquakes to simulate worst case scenarios.

## **ACKNOWLEDGEMENTS**

I would like to express my sincere gratitude to my supervisor Dr. Hiroe MIYAKE and my advisors Drs. Toshiaki YOKOI and Takumi HAYASHIDA for their continuous support, valuable suggestion, and exquisite instructions during this research work.

## **REFERENCES**

- Gansser A., 1964, *Geology of the Himalayas*, Interscience, New York 289.
- Molnar P. and W.P. Chen, 1982, *Mountain Building Processes*, Academic, New York, 41–57.
- Khatti, K. N., 1999, *Himalayan Geology* 20, 1-46.
- Bilham, R., and V. K. Gaur, 2000, *Current Science*, 79, 2000.
- Bilham, R., and K. Wallace, 2005, *Geological Survey of India* 85, 1-14.
- Gupta H. and V.K. Gahalaut, 2014, *Gondwana Res.* 25, 204–213.
- Irikura, K., 1986, *Proc. 7th Japan Earthquake Engineering Symposium*, 151-156.
- Irikura, K., and H. Miyake, 2011, *Pure and Applied Geophysics*, 168, 85-104.
- Irikura, K., T. Kagawa, and H. Sekiguchi, 1997, *Program and abstracts of Seism. Soc. Japan* 2, B25.
- Sharma, M.L., J. Douglas, H. Bungum, J. Kotadia, 2009, *J. Earthquake Eng.* 13, 1191–1210.
- Somerville, P.G., K. Irikura, R. Graves, S. Sawada, D. Wald, N. Abrahamson, Y. Iwasaki, T. Kagawa, N. Smith, and A. Kowada, 1999, *Seismological Research Letters* 70, 59-80.
- Miyake, H., Iwata, T., and Irikura, K., 2003, *Bull Seismol Soc Am*, 93, 2531–2545.